CRYSTAL GROWTH & DESIGN

Article

pubs.acs.org/crystal

NMR Crystallography Comparative Studies of Chiral (1*R*,2*S*,3*R*,5*R*)-3-Amino-6,6-dimethylbicyclo[3.1.1]heptan-2-ol and Its *p*-Toluenesulfonamide Derivative

Magdalena Jaworska,*[,†] Tomasz Pawlak,[†] Rafał Kruszyński,[‡] Marta Ćwiklińska,[§] and Marek Krzemiński[§]

[†]Centre of Molecular and Macromolecular Studies, Polish Academy of Sciences, Sienkiewicza 112, 90-363 Lodz, Poland

[‡]Department of X-ray Crystallography and Crystal Chemistry, Institute of General and Ecological Chemistry, Technical University of Lodz, Zeromskiego 116, 90-924 Lodz, Poland

[§]Department Organic Chemistry, Faculty of Chemistry, Nicolaus Copernicus University, Gagarina 7, 87-100 Torun, Poland

Supporting Information

ABSTRACT: The crystal structure of (1*R*,2*S*,3*R*,5*R*)-3-amino-6,6-dimethyl-2-hydroxybicyclo[3.1.1]heptane **1** was determined and it is presented in reference to the structure of (1*R*,2*S*,3*R*,5*R*)-3-(*p*-tosylamino)-6,6-dimethyl-2-hydroxybicyclo[3.1.1]heptane **2**. ^{1}H and ^{13}C chemical shifts parameters for both structures and for whole unit cells were calculated by using the GIPAW (gauge including projector augmented waves) method. Theoretically calculated chemical shift tensor parameters were verified by ^{13}C CP MAS, 2D PASS, and ^{13}C−^{1}H FSLG HETCOR results to obtain a full structural assignment for ^{13}C and ^{1}H resonances in the solid-state. PISEMA MAS experiment was performed to determine the molecular dynamics of aminoalcohol **1**. The comparison of two structures, obtained after all-atom positions optimization after the GIPAW calculations, revealed small conformational differences consistent with the single-crystal X-ray diffraction results.

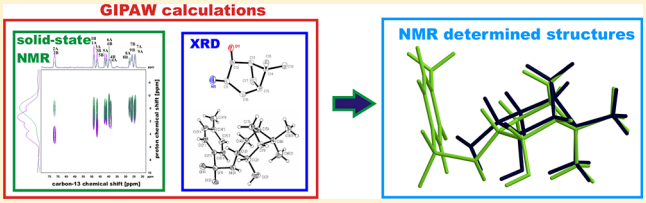

1. INTRODUCTION

Nowadays, pure chiral aminoalcohols play a key role in many branches of human life since they are widely applied as starting materials for the total syntheses of natural products or drugs. Moreover, a large number of them exhibit a wide range of bioactivities, such as antimalarial,[1] antiplasmodial,[2] antiproliferative,[2] antileishmanial,[3] and antimicrobial.[4] Recent studies have also showed a potential ability of aminoalcohols to be the anticancer agents.[5] However, optically active aminoalcohols and their derivatives have been utilized successfully in widespread modern asymmetric syntheses, including the asymmetric addition of diethylzinc to aldehydes,[6,7] the enantioselective Michael addition,[8] the catalytic asymmetric transfer hydrogenation,[9] and the asymmetric synthesis of sulfonamides.[10] This class of compounds is also used as a main source of chirality in the structure of organoboron catalysts, such as oxazaborolidines[11,12] and spiroborate esters[13,14] used in asymmetric borane reduction of C═O[12−15] and C═N double bonds.[15]

Several strategies for the synthesis of chiral aminoalcohols have been reported in the literature, for instance, the addition of α-hydroxy ketones to imines,[16] aminohydroxylation of olefins,[17] aminolytic kinetic resolution of racemic terminal/trans aromatic epoxides,[18,19] and asymmetric ring-opening of meso-epoxides.[20] However, there is still a large requirement to expand knowledge about new aminoalcohol structures and spatial arrangements, which can help find the proper applications.

NMR crystallography approach has recently become a very important method for structures elucidation.[21] Solid-state NMR spectroscopy combined with the X-ray diffraction (XRD) method and supported by gauge-including projector augmented waves (GIPAW) theoretical calculations has proven to be a powerful tool for the crystal structures determination of biologically active compounds,[22] glasses,[23] and minerals.[24] CP MAS (cross-polarization magic angle spinning) NMR is an ideal method for determining a number of independent molecules in the asymmetric unit cell (Z') via comparison between the number of ^{13}C or ^{15}N resonances and the number of chemically different atoms in the crystal.[25] Although, it should be emphasized that the complete structural assignments of observed ^{13}C resonances to their positions in a crystal structure is still a challenging task. The growing interest in the NMR crystallography method has proven that this method can be used in classical organic chemistry for crystal structure determination, especially when single crystals for classical X-ray diffraction measurements are difficult to obtain. However, it can also be treated as a kind of experimental verification of crystal structures obtained by diffraction methods.[26]

In this article, the structural investigations of (1*R*,2*S*,3*R*,5*R*)-3-amino-6,6-dimethylbicyclo[3.1.1]heptan-2-ol are presented (pinane aminoalcohol, **1**) using NMR crystallography method,

Received: July 9, 2012
Revised: November 9, 2012
Published: November 14, 2012

dx.doi.org/10.1021/cg300940k | *Cryst. Growth Des.* 2012, 12, 5956−5965

and a comparison of the obtained results with (1*R*,2*S*,3*R*,5*R*)-3-(*p*-tosylamino)-6,6-dimethyl-2-hydroxybicyclo[3.1.1]heptane (*p*-toluenesulfonamide **2**) was also undertaken.

2. EXPERIMENTAL SECTION

2.1. Materials. (1*R*,2*S*,3*R*,5*R*)-3-Amino-6,6-dimethylbicyclo-[3.1.1]heptan-2-ol **1** and (1*R*,2*S*,3*R*,5*R*)-3-(*p*-tosylamino)-6,6-dimethyl-2-hydroxybicyclo[3.1.1]heptane **2** were prepared for NMR measurements using literature methods.[12] The aminoalcohol crystals **1** suitable for X-ray diffraction experiment were prepared by crystallization using diethyl ether/pentane (1:1, v/v) as a solvent mixture.

2.2. Solid-State NMR Measurements. The solid-state cross-polarization magic angle spinning (CP MAS) NMR was performed on a 400 MHz Bruker Avance III spectrometer, equipped with a MAS probe head using 4 mm ZrO_2 rotors, at a frequency of 100.61 MHz for ^{13}C. A sample of ^{13}C-labeled tyrosine (Tyr) was used to set the Hartmann–Hahn condition for ^{13}C. The conventional ^{13}C CP/MAS spectra were performed with a proton 90° pulse length of 4 μs, contact time of 2 ms, repetition delay of 3 s, spectral width of 60 kHz, time domain size of 3.5 k data points, and at a 8 kHz spinning rate. The acquisition was collected with a SPINAL decoupling sequence.[27] The $^{13}C-^{1}H$ FSLG HETCOR experiments were recorded with a proton 90° pulse length of 2.5 μs, contact time of 50 or 1000 μs, repetition delay of 3 s, time domain size of 1024 data points in F2, and 64 data points in F1, at a 13 kHz spinning rate (standard literature parameters were used).[28] The $^{13}C-^{1}H$ PISEMA MAS experiment was recorded with a proton 90° pulse length of 5 μs at CP, a proton 90° pulse length of 2.5 μs at SEMA, contact time of 1000 μs, repetition delay of 3 s, time domain size of 1024 data points in F2, and 64 data points in F1, at ambient temperature and a 13 kHz spinning rate.[29]

2.3. Crystal Structure Determination. The prism crystal of (1*R*,2*S*,3*R*,5*R*)-3-amino-6,6-dimethyl-2-hydroxybicyclo[3.1.1]heptane **1** was sealed in a glass capillary filled with helium, and next, it was mounted on a KM-4-CCD automatic diffractometer equipped with CCD detector, and used for data collection. X-ray intensity data were collected with graphite monochromated CuK_α (λ = 1.54178 A) radiation at temperature 100(1) K, with ω scan mode. The 22 s exposure time was used, and reflections inside Ewald sphere were collected up to θ = 68°. The unit cell parameters were determined from 6973 strongest reflections. Details concerning crystal data and refinement are given in Table S1 (Supporting Information). Examination of reflections on two reference frames monitored after each 20 frames measured showed no loss of the intensity during measurement. During the data reduction, Lorentz, polarization, and numerical absorption[30] corrections were applied. The structure was solved by direct methods. All the non-hydrogen atoms were refined anisotropically using full-matrix, least-squares technique on F^2. All the hydrogen atoms were found from difference Fourier synthesis after four cycles of anisotropic refinement, and refined as riding on the adjacent atom, with geometric idealization of carbon-bonded atoms after each cycle of refinement and individual isotropic displacement factors equal to 1.2 times the value of equivalent displacement factor of the parent carbon atoms and 1.5 times the parent oxygen and nitrogen atoms. The hydroxyl and amine groups were allowed to rotate about the O–C and N–C bond axes, respectively. The Flack parameter was refined as full matrix parameter. The SHELXS97, SHELXL97, and SHELXTL[31] programs were used for all the calculations. Atomic scattering factors were those incorporated in the computer programs. Selected interatomic bond distances and angles are listed in Table 1 and intermolecular interactions are listed in Table 2.

Tables of crystal data and structure refinement, anisotropic displacement coefficients, atomic coordinates, and equivalent isotropic displacement parameters for non-hydrogen atoms, H-atom coordinates and isotropic displacement parameters, bond lengths, and interbond angles have been deposited with the Cambridge Crystallographic Data Centre under No. CCDC885739.

2.4. QM Calculations. The quantum chemical calculations were made using the CASTEP[32] program. Geometry optimizations were performed with staring models based on the XRD-determined crystal structures of **1** and **2**, and the generalized density approximation DFT functional PBE[33] was applied. A comparison of the average forces remaining on the atoms after geometry optimization was carried out for all-atom optimizations by using a maximum planewave cutoff energy of 550 eV and an ultrasoft pseudopotential,[34] and a 1 × 2 × 1 Monkhorst–Pack grid[35] was used to sample the Brillouin zone. The unit cell parameters for structures **1** and **2** were taken from the experimental data.[12] The NMR chemical shifts were computed by the use of the GIPAW (gauge including projector augmented waves) method.[36] The calculations upon the full crystal structure used a planewave basis set with a maximum cutoff energy of 550 eV.

2.5. NMR Chemical Shift Tensors. To avoid any unnecessary errors, the calculated shifts were arbitrarily referenced by fitting the calculated shieldings as a function of the experimental shift value by a straight line of slope −1 (the intercept thus being the only variable). The chemical shifts have been calculated by using equation $\delta_i = \sigma_{REF} - \sigma_i$, where σ_{REF} is the intercept determinant from correlation between experimental δ_{iso} and theoretical σ_{iso} parameters and minimization of RMSD value. The same σ_{REF} value was used to recalculate σ_{ii} into δ_{ii} parameters. The reference value is then extracted from the intercept of the best fit. This requires preliminary assignment, which was proposed from first-principles calculations discussed further below. All numerical data are presented in the Supporting Information.

Table 1. Selected Distances and Torsion Angles within Compound 1 [Å, deg]

N1—C1	1.4689(19)	N11—C11	1.468(2)
O1—C2	1.4190(18)	O11—C12	1.4108(18)
C1—C2—C3—C4	−59.98(15)	C11—C12—C13—C14	−58.24(16)
C2—C3—C4—C5	81.24(13)	C12—C13—C14—C15	82.10(13)
C3—C4—C5—C6	−82.71(12)	C13—C14—C15—C16	−83.08(13)
C4—C5—C6—C1	65.52(16)	C14—C15—C16—C11	63.37(17)
C5—C6—C1—C2	−29.79(18)	C15—C16—C11—C12	−25.93(19)
C6—C1—C2—C3	26.94(16)	C16—C11—C12—C13	23.30(17)
C1—C2—C3—C7	34.91(15)	C11—C12—C13—C17	36.91(15)
C2—C3—C7—C5	−85.73(12)	C12—C13—C17—C15	−86.78(12)
C3—C7—C5—C6	82.72(13)	C13—C17—C15—C16	83.60(14)
C7—C5—C6—C1	−29.32(17)	C17—C15—C16—C11	−31.70(18)

Table 2. Hydrogen Bonds Geometry of Compound 1 [Å, deg]

D–H···A	*d*(D–H)	*d*(H···A)	*d*(D···A)	∠(DHA)
N1–H1N···O1[a]	0.91	2.59	3.4864(19)	165.1
O1–H1O···N11	0.86	1.9	2.7579(15)	170.5
N11–H11N···O11	0.84	2.40	2.744(2)	105.4
O11–H11O···N1	0.80	2.03	2.8113(16)	167.2
C8–H8B···O1	0.98	2.40	2.8895(16)	110.6
C18–H18B···O11	0.98	2.43	2.9003(16)	109.3

[a]Symmetry transformations used to generate equivalent atoms: (i) x, y +1, z.

3. RESULTS AND DISCUSSION

NMR crystallography protocol used for structure resolving was based on the schematic routine presented elsewhere.[37] The procedure used in this article is presented in Scheme 1.

dx.doi.org/10.1021/cg300940k | *Cryst. Growth Des.* 2012, 12, 5956–5965

Scheme 1. Employed NMR Crystallography Protocol

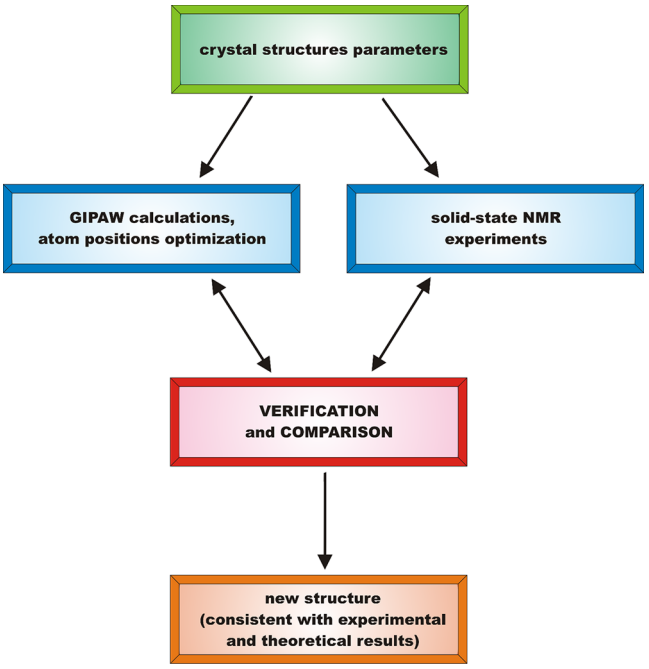

At the beginning, the crystal structure of **1** has been determined and compared with **2**. Next, the ^{13}C CP MAS NMR data were used for preliminary structural assignments of measured ^{13}C chemical shifts, and simultaneously, the GIPAW theoretical calculations of shielding parameters based on X-ray structure of aminoalcohol **1** (Figure 1) and *p*-

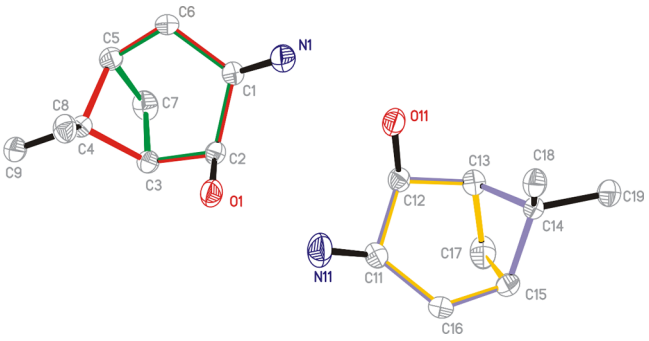

Figure 1. Molecular structure of compound **1** with atom numbering scheme, plotted with 50% probability of displacement ellipsoids. The hydrogen atoms were omitted for clarity. For description of colors, see text.

toluenesulfonamide derivative **2**[12] were performed. The final ^{13}C chemical shift assignments were completed by $^{13}C-^{1}H$ FSLG HETCOR and PISEMA MAS experiments to show the high accuracy of theoretical and experimental data and to describe the molecular dynamics of investigated compounds. At the end, two calculated and consistent with NMR results structures of **1** and **2** have been compared.

3.1. Comparison of (1*R*,2*S*,3*R*,5*R*)-3-Amino-6,6-dimethylbicyclo[3.1.1]heptan-2-ol 1 and (1*R*,2*S*,3*R*,5*R*)-3-(*p*-Tosylamino)-6,6-dimethyl-2-hydroxybicyclo[3.1.1]-heptane 2 Crystal Structures. In the solid state, the aminoalcohol **1** crystallizes with two molecules in the asymmetric unit, in opposition to the crystal structure of tosylate **2**,[12] which has only one molecule in the asymmetric unit. A perspective view of the compound **1** structure is shown in Figure 1.

All atoms of compound **1** occupy the general positions. The asymmetric part of the unit cell contains the two molecules of **1**, related by noncrystallographic pseudosymmetry 2-fold axis. In general, the molecules possess similar conformations (Table 1) with the weighted root-mean-square deviation of superimposed non-hydrogen atoms of both molecules equal to 0.049 Å (the N1 and N11 are the most deviating atoms and are separated by the distance of 0.111 Å).

The cyclic parts of the molecules are almost identical with the root-mean-square deviation of superimposed carbon atoms of both molecules equal to 0.016 Å. The molecules possess configurations *R*, *S*, *R*, and *R* of C1, C2, C3, and C5 atoms, respectively, and of C11, C12, C13, and C15 atoms, respectively. The total puckering amplitudes[38] of the six -membered rings are 0.7491, 0.7512, 0.9268, and 0.9108 Å, respectively, for rings containing C1/C2/C3/C4/C5/C6 (ring A, marked red in Figure 1), C11/C12/C13/C14/C15/C16 (ring B, marked violet in Figure 1), C1/C2/C3/C7/C5/C6 (ring C, marked green in Figure 1), and C11/C12/C13/C17/C15/C16 (ring D, marked orange in Figure 1) atoms. The first two (A and B) of these four rings possess the chair conformations (the succeeding torsion angles of the rings adopts alternate signs, and the smallest C_s asymmetry parameters[39] are 3.70 and 3.38° for planes going through the C1···C4 and C11···C14 atoms, respectively), and the second two rings (C and D) possess the boat conformations (the succeeding torsion angles of the rings adopts +, +, −, −, +, − signs, and the smallest C_s asymmetry parameters are 4.02 and 3.83° for mirror planes passing through the C1···C7 and C11···C17 atoms, respectively).

The conformation and configuration of **1** resemble those one existing in (1*R*,2*S*,3*R*,5*R*)-3-(*p*-tosylamino)-6,6-dimethyl-2-hydroxybicyclo[3.1.1]heptane **2**,[12] i.e., the **1** substituted by tosyl group at the amine nitrogen atom, and is opposite to 2,6,6,-trimethyl-3-(2,9,9-trimethyl-3-oxa-5-azatricyclo-[6.1.1.$0^{2,6}$]dec-5-yl)bicyclo[3.1.1]heptan-2-ol containing the three fused cyclic rings.[40] The superimposed non-hydrogen atoms of any molecule of **1** and **2** deviate no more than 0.11 Å, and weighted root-mean-square deviation for all these atoms is smaller than 0.05 Å.

The both molecules occupying the asymmetric unit are assembled together by the O−H···N hydrogen bonds (Table 2) forming $R_2^2(10)$ motifs. The long N−H···O intermolecular contact (Table 2), which can be classified as a weak hydrogen bond,[41] expands the hydrogen bonded dimers to the supramolecular chain extending along crystallographic [010] axis and described by basic C(5) graph.

The conformations of molecules of **1** are additionally stabilized by the weak N/C−H···O hydrogen bonds. The presence of the three relatively strong and multiple weak hydrogen bond donors and only two hydrogen bonds acceptors leads to complete saturation of the acceptors by two interactions and existence of one noninteracting strong hydrogen bond donor per molecule. The discussion about hydrogen bond is extremely important in the determination of structure using solid-state NMR methods. Yates et al.[42] have already presented a strong sensitivity of chemical shift parameters calculated by GIPAW method on the hydrogen bond in maltose anomers including also directionality of this interaction.

dx.doi.org/10.1021/cg300940k | *Cryst. Growth Des.* 2012, 12, 5956−5965

3.2. Complete ^{13}C Chemical Shift Assignment for Aminoalcohol 1 and *p*-Tolunensulfonamide 2. For both compounds, **1** and **2**, the standard solid-state ^{13}C CP MAS and ^{13}C CP DD (dipolar dephasing)[43] MAS NMR was performed, as well as solution-NMR experiments were made (see Supporting Information) to obtain preliminary assignments for aminoalhohol **1** and *p*-toluenesulfonamide **2**. On the basis of the crystal structures, the GIPAW calculation of NMR parameters were made for fully optimized structures of two investigated compounds. Calculation results were compared with the experimental ones (Table 3), and the absolute assignments of ^{13}C carbon resonances in the solid-state for aminoalcohol **1** and *p*-toluenesulfonamide **2** were presented on Figures 2 and 3.

Table 3. Experimental and Calculated (GIPAW) ^{13}C δ_{iso} for Aminoalkohol 1 and *p*-Toluenesulfonamide 2

aminoalcohol **1**			*p*-toluenesulfonamide **2**		
nucleus[a]	δ_{iso} exptl[b]	δ_{iso} calcd[c]	nucleus	δ_{iso} exptl[b]	δ_{iso} calcd[c]
3A	47.4	50.0	3	47.0	47.6
2A	72.6	77.6	2	74.8	78.8
1A	48.9	47.9	1	47.9	43.9
6A	40.5	39.9	6	39.7	39.4
5A	41.8	41.5	5	33.5	31.0
4A	39.9	38.8	4	38.9	36.6
7A	26.4	23.5	7	25.6	22.3
9A	24.8	24.8	9	26.0	24.7
8A	27.5	25.2	8	27.4	27.4
3B	47.4	48.9	10	21.8	19.1
2B	73.1	75.1	3′ and 5′	127.2	132.4
1B	49.3	50.0	2′ and 6′	130.3	126.9
6B	40.5	41.3	1′	138.5	142.7
5B	42.7	41.4	4′	144.2	147.5
4B	39.4	39.7			
7B	25.1	27.0			
9B	26.4	23.1			
8B	28.3	26.1			

[a]Compound **1** crystallizes with two molecules in the asymmetric unit, and the results are presented for two molecules: A and B. [b]As determined from ^{13}C CP MAS NMR spectrum (Figures 1 and 2) and based on ^{13}C NMR in liquid (see Supporting Information). [c]Calculations for the full crystal structure and the chemical shifts have been calculated using equation $\delta_i = \sigma_{REF} - \sigma_i$, where σ_{REF} is the intercept, determinant from the correlation between experimental δ_{iso} and theoretical σ_{iso} parameters and minimization of root-mean-square deviation (RMSD) value (see Supporting Information).

Most of the ^{13}C resonances of **1** are doubled (Figure 2) due to crystallization of **1** with two molecules in the asymmetric unit. A full resolution of resonances for C-6 and C-3 could not be observed. On the contrary, the **2** crystallizes with only one molecule in the asymmetric unit, and only one signal for each carbon is observed (Figure 3). On the ^{13}C CP DD MAS NMR spectra, all signals from CH and CH_2 groups were effectively suppressed for both compounds, and only quaternary and methyl group signals are observed.[30]

The absolute assignments of ^{13}C carbon resonances were based on the computation results (GIPAW), which were compared with isotropic chemical shifts and anisotropic values of chemical shift tensor (CST) for each of the ^{13}C nuclei to gain the best adjustment between theory and experiment. CST parameters were obtained from the analysis of spinning sideband intensities.[44] The 2D PASS sequence for analysis of CST for ^{13}C nuclei were used because this technique offers good sensitivity without overlapping the sideband systems in comparison to other methods.[45] For both investigated compounds, the 2D PASS spectra were recorded at 1.2 kHz spinning rate. Using proper data shearing, for each nuclei, the spinning sideband systems were separated, and the ^{13}C δ_{ii} parameters were fitted using TOPSPIN.[46] Additionally, the span Ω and skew κ, that represent the chemical shift anisotropy and the asymmetry of electron distribution around each ^{13}C nuclei, respectively, have been also presented. All experimental CST parameters are listed in Tables 4 and 5.

The δ_{iso} experimental values for ^{13}C nuclei in the bicyclic ring of the aminoalcohol and *p*-toluenesulfonamide (C, 1−9) showed only small differences. In fact, the largest difference was observed for C-5 (CH); in **2**, the δ_{iso} was shifted upfield at about 9 ppm. However, more significant differences were noted in the case of δ_{22} and δ_{33} values for C-8 (CH_3), C-3 (CH-N), C-1 (CH), and C-4 (CH). For both structures, the carbon resonances specified above are sensitive to the electron distribution changes related to the different hydrogen bonding and slight conformational changes of aminoalcohol **1** and *p*-toluenesulfonamide **2** bicyclic rings as it was found by X-ray diffraction analysis. The other parameter that varies (also slightly) is span parameter Ω. Small differences between Ω is also probably connected with the changes in intra- and intermolecular dynamics, differences of short contacts between molecules in the crystal or between unit cell dimensions for both structures.

Calculated ^{13}C CST parameters showed good agreement with unscaled GIPAW calculated results for both investigated compounds (Tables 4 and 5), and only minor differences were noted due to the imperfection of the experimental technique and theoretical calculation methods. The calculation results for **1** and **2** are visualized as correlation curves (Figure 4) between theoretical and experimental NMR parameters for chemical shift isotropic values (δ_{iso}), principal components of chemical shift tensor (δ_{11}, δ_{22}, and δ_{33}), and span ($\Omega = \delta_{11}-\delta_{33}$) parameter.

The slope of the correlation curves (Figure 4) is not the ideal −1.000 and could cause some problems with the comparison of experimental and computed results, what are not unusual for the GIPAW method.[47,22b] For both structures, the root-mean-square deviation (RMSD) between experimental and scaled computed data was 2.12 and 3.67 for **1** and **2**, respectively.

Additionally, on ^{15}N CP MAS, the following isotropic chemical shift have been observed for **1**, 33.63 and 37.02 ppm, and for **2**, 109.97 ppm (see Supporting Information, Figure S1). ^{15}N δ_{iso} values obtained from GIPAW calculations for aminoalcohol differed by 5 ppm in comparison to measured ones, and the values obtained for *p*-toluenesulfonamide differed by 75−80 ppm in reference to theoretical and experimental values obtained for aminoalcohol. The comparison between theoretical and experimental results indicated that GIPAW calculations have high accuracy.

The most important advantage of the GIPAW calculations method lies in the robust prediction of ^{1}H isotropic chemical shifts. Because of its characteristics, the XRD method does not guarantee the precise designation of proton positions. The main advantage of NMR crystallography method in the comparison to classical X-ray diffraction analysis is the fact that using NMR technique combined with advanced CST calculation one can clearly obtain a high accuracy of protons

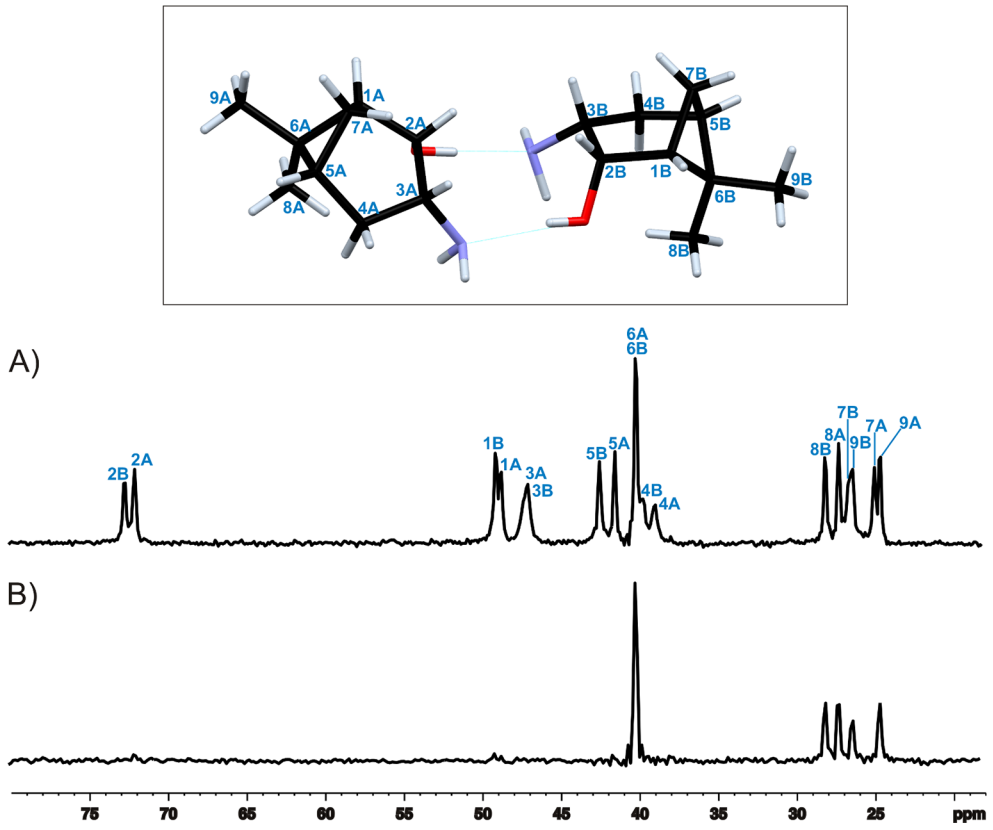

Figure 2. (A) ^{13}C CP MAS NMR spectrum of aminoalcohol **1** with full structural assignments; (B) ^{13}C CP DD MAS NMR spectrum of **1**. Both spectra were recorded with 8 kHz spinning rate.

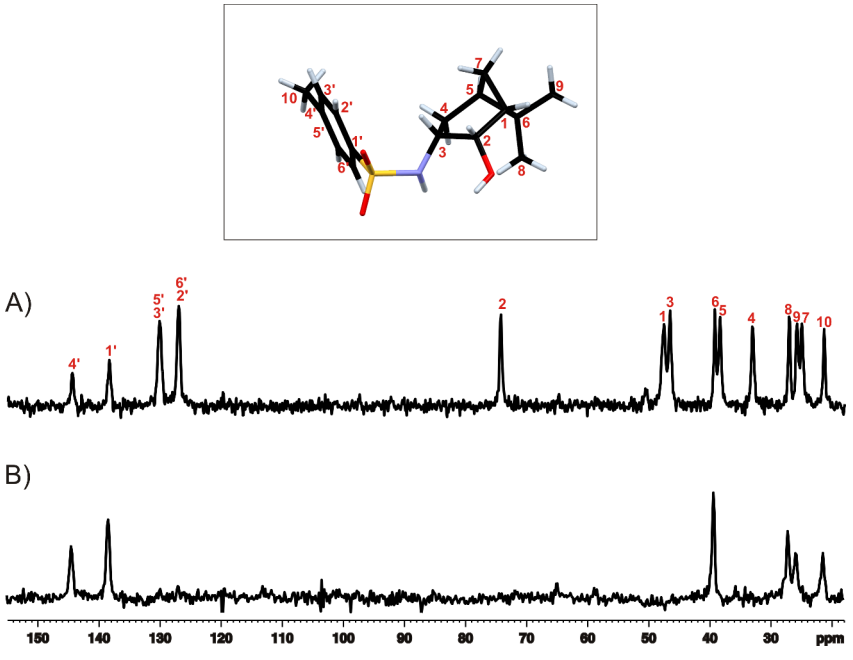

Figure 3. (A) ^{13}C CP MAS NMR spectrum of *p*-toluenesulfonamide **2** with full structural assignments; (B) ^{13}C CP DD MAS NMR spectrum of **2**. Both spectra were recorded with 8 kHz spinning rate.

position determination. Solid-state NMR experiments provide detailed information about interactions between different nuclei, e.g., ^{1}H and ^{13}C to obtain structural assignment of high accuracy. The computed and experimental solid-state proton isotropic chemical shifts for **1** are listed in Table 6.

The experimental values of ^{1}H isotropic chemical shift were determined from $^{13}C-^{1}H$ HETCOR spectrum of **1**, with the usage of the FSLG ^{1}H decoupling,[48] presented in Figure 5. Herein, the short contact time of 50 μs was implemented to observe correlations of carbons directly bonded to protons. Additionally, $^{13}C-^{1}H$ FSLG HETCOR experiment with longer

dx.doi.org/10.1021/cg300940k | *Cryst. Growth Des.* 2012, 12, 5956−5965

Table 4. ^{13}C δ_{ii} Parameters[a] for Aminoalkohol Obtained from 2D PASS Experiment

nucleus	δ_{iso} (ppm)	δ_{11}	δ_{22}	δ_{33}	Ω	κ
3A	47.4	58.4	56.4	27.4	31.0	0.87
2A	72.6	88.7	85.4	43.8	44.9	0.85
1A	49.0	60.0	44.0	42.9	17.2	−0.87
6A	40.5	54.9	34.0	32.4	22.5	−0.86
5A	41.7	56.3	35.3	33.6	22.7	−0.85
4A	39.9	58.9	31.2	29.4	29.4	−0.88
7A	26.4	34.8	33.3	11.2	23.6	0.88
9A	24.8	32.9	31.0	10.4	22.5	0.84
8A	27.5	40.2	37.9	4.41	35.8	0.87
3B	47.4	58.4	56.4	27.4	31.0	0.87
2B	73.1	88.2	85.3	45.7	42.7	0.86
1B	49.3	58.8	45.1	44.1	14.7	−0.85
6B	40.5	54.9	34.0	32.4	22.5	−0.86
5B	42.7	51.4	49.0	26.9	24.6	0.86
4B	39.4	61.4	29.2	27.7	33.7	−0.91
7B	25.1	33.1	31.4	11.0	22.1	0.85
9B	26.4	34.8	33.3	11.2	23.6	0.88
8B	28.3	40.4	37.8	9.8	33.5	0.85

[a]The ^{13}C δ_{ii} parameters are defined as follows: $\delta_{11} \geq \delta_{22} \geq \delta_{33}$. The estimated error in δ_{11}, δ_{22}, and δ_{33} is 3 ppm, $\delta_{iso} = (\delta_{11} + \delta_{22} + \delta_{33})/3$; span is expressed as $\Omega = \delta_{11} - \delta_{33}$; and skew is expressed as $\kappa = 3(\delta_{22} - \delta_{iso})/\Omega$.

Table 5. ^{13}C δ_{ii} Parameters[a] for *p*-Toluenesulfonamide Obtained from 2D PASS Experiment

nucleus	δ_{iso} (ppm)	δ_{11}	δ_{22}	δ_{33}	Ω	κ
3	47.0	58.0	42.0	40.9	17.2	−0.87
2	74.8	90.6	90.6	43.2	47.4	1.00
1	47.9	65.9	53.9	23.9	42.0	0.43
6	39.7	56.0	32.5	30.7	25.3	−0.86
5	33.5	53.16	24.7	22.6	30.5	−0.86
4	38.9	46.5	44.9	25.3	21.2	0.85
7	25.6	41.6	18.4	16.8	24.8	−0.87
9	26.0	34.6	32.9	10.4	24.3	0.86
8	27.4	48.7	16.7	32.0	16.7	−1.00
10	21.8	30.1	28.5	6.7	23.4	0.87
3′ and 5′	127.2	214.3	153.5	13.9	200.5	0.39
2′ and 6′	130.3	224.9	144.3	24.5	200.4	0.20
1′	138.5	201.6	161.1	54.7	147.0	0.45
4′	144.2	246.5	176.6	9.9	236.5	0.41

[a]The ^{13}C δ_{ii} parameters are defined as follows: $\delta_{11} \geq \delta_{22} \geq \delta_{33}$. The estimated error in δ_{11}, δ_{22}, and δ_{33} is 3 ppm, $\delta_{iso} = (\delta_{11} + \delta_{22} + \delta_{33})/3$; span is expressed as $\Omega=\delta_{11} - \delta_{33}$; and skew is expressed as $\kappa = 3(\delta_{22} - \delta_{iso})/\Omega$.

contact time (1000 μs) have also been recorded to show correlations between carbons and neighboring protons not directly bonded to carbons. A comparison between two $^{13}C-^{1}H$ FSLG HETCOR spectra recorded with different contact times is presented in the Figure 6.

The correlation peak between carbon 2 and protons from methyl group 8 are exhibited clearly (Figure 6, green-colored spectrum), and this is in agreement with the XRD measurements and calculations results (Figure 1 and 2). The calculation results for δ_{iso} ^{13}C of 3A, 3B and 2A, 2B deviate from the experimental data (Figure 5). Carbons mentioned here participate in a strong intermolecular hydrogen bonding between two molecules of aminoalcohol **1**, as it was proved by XRD measurements, and this probably has an influence on differences between calculated and experimental results. However, the computed results differed by only ∼5 ppm (for ^{13}C) from experimental ones, what is obviously an evidence of good agreement between the computed structure and NMR measurements.

In conclusion, for (1*R*,2*S*,3*R*,5*R*)-3-amino-6,6-dimethylbicyclo[3.1.1]heptan-2-ol **1** and (1*R*,2*S*,3*R*,5*R*)-3(*p*-tosylamino)-6,6-dimethyl-2-hydroxybicyclo[3.1.1]heptane **2**, the 2D PASS and $^{13}C-^{1}H$ FSLG HETCOR experiments in combination with the GIPAW CST calculations for full crystal structures allowed to find a complete structural assignment and determination of the new structures in the solid-state.

3.3. Analysis of the Molecular Dynamics for 1. Molecular dynamics strongly affect and complicate the theoretical calculations of the chemical shifts in the solid state.[49] The existence and the spatial range of small amplitude disorder in solid-state phase have a significant influence on chemical shift calculations.[50] For analysis of the effect of molecular motion on the line shape of the dipolar spectra, a modified sequence of 2D PISEMA MAS has been employed, as previously reported.[31] The polarization inversion spin exchange at the magic angle (PISEMA) pulse sequence has been recently used to measure $^{1}H-^{13}C$ dipolar couplings in the solid samples.[51] The main advantage of this technique is its high tolerance for RF inhomogeneity, and it makes possible an accurate determination of $^{13}C-^{1}H$ dipolar interactions. The 2D PISEMA MAS spectrum of **1** was recorded with a spinning rate of 13 kHz, and the F1 slices with labeled example splitting between the singularities of the doublets reflected to the dipolar couplings of CH (2A and 2B) and CH_3 (8A and 8B) carbons are presented in Figure 7.

If the r_{ij} $^{13}C-^{1}H$ distance is equal to 1.07 Å, the dipolar coupling constant δ for the rigid-limit is 24.0 kHz. However, the exact Hartmann−Hahn matching condition yields a maximum scaling factor (sf) of ∼0.580 (cos 54.7°), and for the rigid system, the δ constant value is about 14.0 kHz (24 kHz × 0.580). For the CH_3 group, the dipolar coupling at about 4 kHz clearly appeared in the spectrum. The reduce value of the dipolar coupling originates from fast rotations of methyl groups. For the rigid CH group, the heteronuclear dipolar splitting pattern looks similar to the Pake pattern[52] with dipolar splitting value of 14 kHz originating from its strong $^{13}C-^{1}H$ dipolar interactions. The comparison of results of the GIPAW calculations of CH_3 groups chemical shift parameters with the results obtained from 2D PISEMA MAS allows noticing that experimental parameters and theoretical assumptions are consistent. A lack of deviations of computed CST parameters proves the high accuracy of the GIPAW computation method.

3.4. Comparison of (1*R*,2*S*,3*R*,5*R*)-3-Amino-6,6-dimethylbicyclo[3.1.1]heptan-2-ol 1 and (1*R*,2*S*,3*R*,5*R*)-3(*p*-Tosylamino)-6,6-dimethyl-2-hydroxybicyclo[3.1.1]-heptane 2 NMR Structures. The comparison by superimposition of two structures obtained after all-atom positions optimization during the GIPAW calculations is presented in Figure 8 .

It should be noted that only slight differences between structures of **1** and **2** are in the conformation of the bicyclic ring in the region containing carbon atoms 1−4. The observed changes are consistent with the XRD results and are caused by different hydrogen bonding interactions in both structures. The other reasons of differences are the following: (1) in the crystal structure of **2**, the unit cell is bigger than in **1**, and (2) the

dx.doi.org/10.1021/cg300940k | Cryst. Growth Des. 2012, 12, 5956−5965

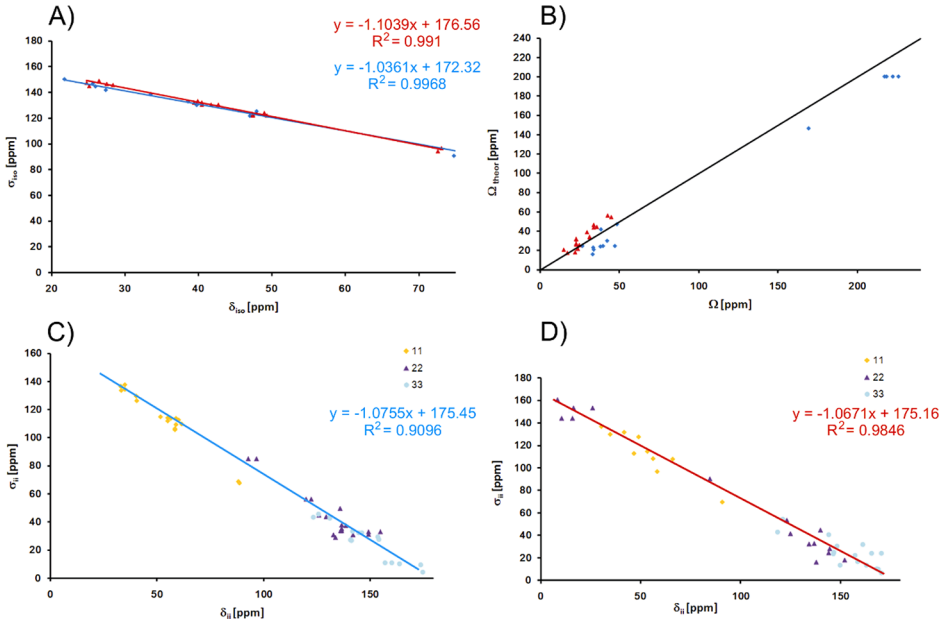

Figure 4. Correlation between experimental and unscaled calculated (GIPAW) ^{13}C CST parameters for **1** and **2**: (A) δ_{iso} (**1** (blue) and **2** (red)); (B) $\Omega = \delta_{11} - \delta_{33}$ (span), (**1** (red) and **2** (blue); black line represents the ideal correlation of $\Omega_{exptl} = \Omega_{calcd}$); (C) δ_{ii} (δ_{11}, orange; δ_{22}, violet; δ_{33}, light blue) for the aminoalcohol **1**; (D) δ_{ii} (δ_{11}, orange; δ_{22}, violet; δ_{33}, light blue) for *p*-toluenesulfonamide **2**.

Table 6. Experimental and Calculated (GIPAW) ^{1}H δ_{iso} for Aminoalcohol 1

nucleus[a]	δ_{iso} exptl[b]	δ_{iso} calcd[c]
9A	−0.217	0.00
7A	0.125	0.62
8A	0.125	−0.24
4A	0.93	0.50
5A	0.93	0.77
7′A	0.125	0.62
1A	1.36	1.07
4′A	0.93	0.50
3A	2.58	2.14
2A	4.16	3.65
9B	−0.29	0.01
7B	−0.29	0.61
8B	−0.29	−0.18
4B	0.93	0.85
5B	0.93	0.99
7′B	−0.29	0.61
1B	1.36	1.17
4′B	0.93	0.85
3B	2.58	2.46
2B	4.16	3.85

[a]Numbering system of carbons in **1**. [b]As determined from ^{13}C−^{1}H FSLG HETCOR spectrum (Figure 5). [c]Calculations for full crystal structure; the chemical shifts have been calculated using equation $\delta_i = \sigma_{REF} - \sigma_i$, where σ_{REF} is the intercept, determinant from the correlation between experimental δ_{iso} and theoretical σ_{iso} parameters and minimization of root-mean-square deviation (RMSD) value (see Supporting Information).

presence of an aromatic ring can cause the electron distribution changes in the whole molecule.

The presented here protocol for detailed structural studies includes the solid-state NMR results combined with GIPAW calculations of CST parameters that are compared with X-ray diffraction results. The planewave-pseudopotential calculations

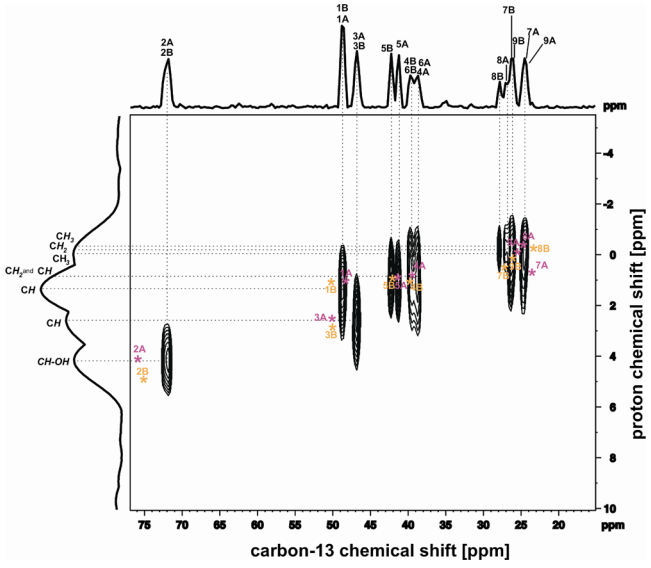

Figure 5. ^{13}C−^{1}H FSLG HETCOR spectrum of **1** recorded at an ^{1}H Larmor frequency of 400 MHz, at 13 kHz spinning rate, and using contact time of 50 μs. The GIPAW computed isotropic ^{1}H and ^{13}C chemical shift (for A and B molecules of **1**) values are marked by violet and orange stars (*).

methods have increased the accuracy of solving structures using only the unit cell parameters and the space group from XRD measurements and solid-state NMR data. The cooperation between diffraction and solid-state NMR methods presented here leads to receiving more precise structural information. The constant improvement of computer analysis of NMR and diffraction data allows a much better understanding of the crystalline state nature.

4. CONCLUSIONS

In this project, the powerful NMR crystallography method has been used for the structural investigations of two compounds.

dx.doi.org/10.1021/cg300940k | *Cryst. Growth Des.* 2012, 12, 5956−5965

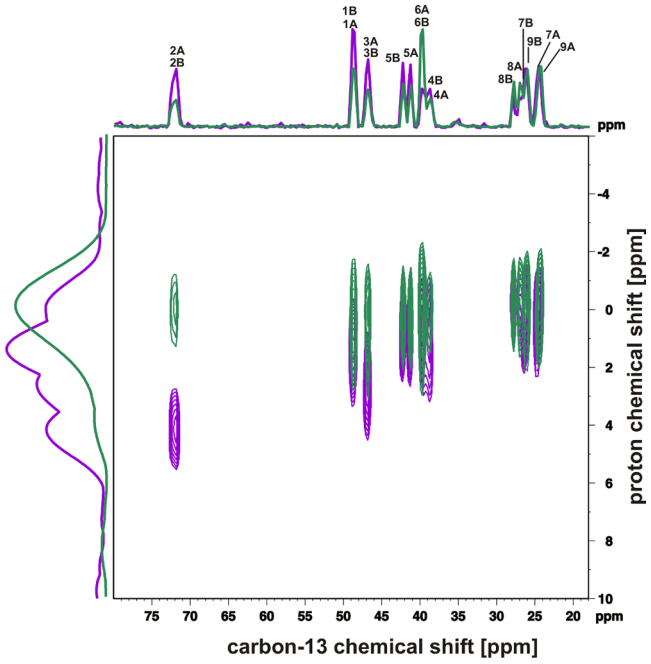

Figure 6. $^{13}C-^{1}H$ FSLG HETCOR spectra of **1** recorded at an ^{1}H Larmor frequency of 400 MHz, at 13 kHz spinning rate, and using different contact time of 50 μs (violet) and 1000 μs (green).

The ^{13}C resonances for the two molecules existing in the asymmetric unit of (1*R*,2*S*,3*R*,5*R*)-3-amino-6,6-dimethylbicyclo[3.1.1]heptan-2-ol **1** and for one molecule present in the asymmetric unit of (1*R*,2*S*,3*R*,5*R*)-3(*p*-tosylamino)-6,6-dimethyl-2-hydroxybicyclo[3.1.1]heptane **2** have been experimentally determined by means of 2D PASS and $^{13}C-^{1}H$ FSLG HETCOR spectra measurements, and a complete structural assignment has been shown after the GIPAW calculations for the fully optimized XRD crystal structure. The comparison between structures of **1** and **2** has revealed only small conformational differences, probably

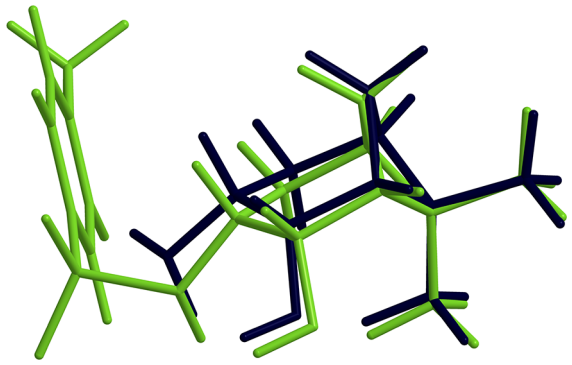

Figure 8. Superimposition of two structures obtained from the GIPAW calculations: black structure represents **1**, and green structure represents **2**.

originating from the variable hydrogen bonding in the crystal lattices. Additionally, for compound **1**, the assignment of ^{1}H resonances based on verification of the CST calculated parameters using the GIPAW method by means of $^{13}C-^{1}H$ FSLG HETCOR experimental results have been proposed. The usefulness of PISEMA MAS experiment for determination of the molecular dynamics of **1** has been shown, and consistence of the experiment with the theoretical assumptions has been proven. The structure determination and assignment of ^{13}C and ^{1}H resonances in the solid-state of aminoalcohol **1** provide a base for further considerations about the structures of oxazaborolidines and spiroborate esters, used as organocatalysts in the modern organic synthesis.

■ ASSOCIATED CONTENT

Supporting Information

Tables of crystal and structure refinement data of compound **1**, GIPAW calculation results for compounds **1** and **2**; Figures of ^{15}N CP MAS NMR spectra of **1** and **2** and correlation curve between experimental and unscaled calculated (GIPAW) ^{1}H δ_{iso} for **1**. Crystallographic Information Files (CIF) for NMR

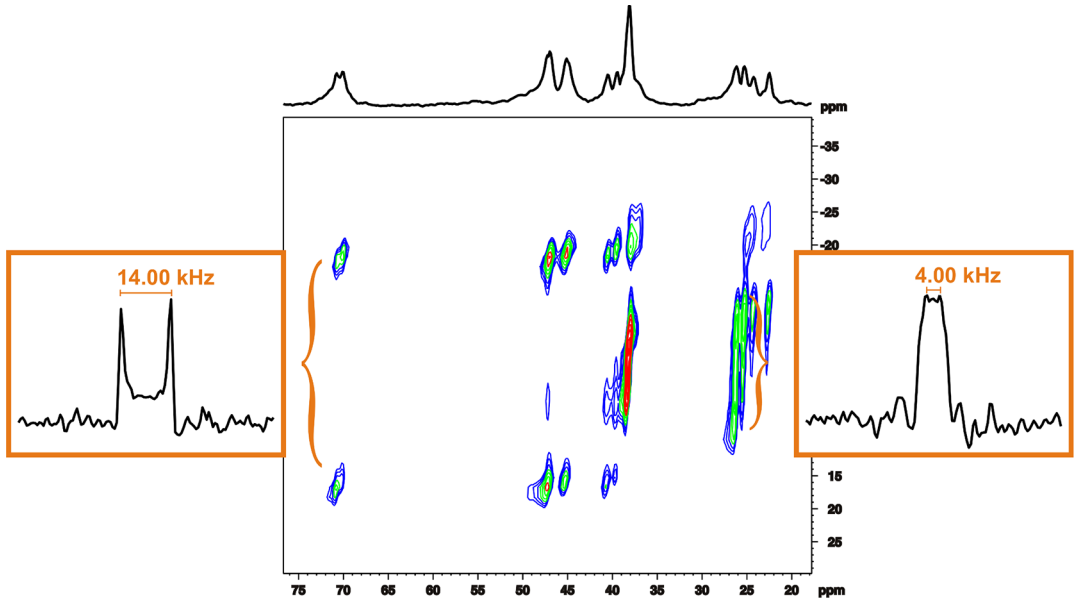

Figure 7. 2D PISEMA MAS spectrum recorded with a 13 kHz spinning rate at ambient temperature for aminoalcohol **1** with F1 slices of CH_3 (carbons 8A and 8B) and CH (carbons 2A and 2B) groups.

dx.doi.org/10.1021/cg300940k | *Cryst. Growth Des.* 2012, 12, 5956−5965

determined structures. This material is available free of charge via the Internet at http://pubs.acs.org.

AUTHOR INFORMATION

Corresponding Author

*Phone: +4842 68 03 308. E-mail: magdajaworska@vp.pl or mjawor@cbmm.lodz.pl.

Notes

The authors declare no competing financial interest.

ACKNOWLEDGMENTS

The crystallographic part was financed by funds allocated by the Ministry of Science and Higher Education to the Institute of General and Ecological Chemistry, Technical University of Lodz. The financial support from the Ministry of Science and Higher Education, Warsaw, grant no 2683/B/H03/2010/38, is acknowledged by M.K.. M.C. is grateful for financial support from the European Social Fund and National Budget, grant "Krok w przyszłość: stypendia dla doktorantów IV edycja 2011/2012". The computational resources were partially provided by the Polish Infrastructure for Supporting Computational Science in the European Research Space (PL-GRID) and ACK CYFRONET AGH grant no. MNiSW/IBM_BC_HS21/CBMMPAN/029/2011.

REFERENCES

(1) Kaur, K.; Jain, M.; Reddy, R. P.; Jain, R. *Eur. J. Med. Chem.* **2010**, *45*, 3245.
(2) Hans, R. H.; Gut, J.; Rosenthal, P. J.; Chibale, K. *Bioorg. Med. Chem. Lett.* **2010**, *20*, 2234.
(3) Coimbra, E. S.; de Almeida, M. V.; Junior, C. O. R.; Taveira, A. F.; da Costa, C. F.; de Almeida, A. C.; Reis, E. F. C.; da Silva, A. D. *Chem. Biol. Drug Des.* **2010**, *75*, 233.
(4) Prasad, A. K.; Kumar, P.; Dhawan, A.; Chhillar, A. K.; Sharma, D.; Yadav, V.; Kumar, M.; Jha, H. N.; Olsen, C. E.; Sharma, G. L.; Parmar, V. S. *Bioorg. Med. Chem. Lett.* **2008**, *18*, 2156.
(5) Bai, B.; Li, X.-Y.; Li, Y.; Zhu, H.-J. *Bioorg. Med. Chem. Lett.* **2011**, *21*, 2302.
(6) Jaworska, M.; Błocka, E.; Kozakiewicz, A.; Wełniak, M. *Tetrahedron: Asymmetry* **2011**, *22*, 648.
(7) Watts, C. C.; Thoniyot, P.; Hirayama, L. C.; Romano, T.; Singaram, B. *Tetrahedron: Asymmetry* **2005**, *16*, 1829.
(8) Yang, W.; Jia, Y.; Du, D.-M. *Org. Biomol. Chem.* **2012**, *10*, 332.
(9) Watts, C. C.; Thoniyot, P.; Cappuccio, F.; Verhagen, J.; Gallagher, B.; Singaram, B. *Tetrahedron: Asymmetry* **2006**, *17*, 1301.
(10) Zhang, Y.; Chitale, S.; Goyal, N.; Li, G.; Han, Z. S.; Shen, S.; Ma, S.; Grinberg, N.; Lee, H.; Lu, B. Z.; Senanayake, C. H. *J. Org. Chem.* **2012**, *77*, 690.
(11) Corey, E. J.; Helal, C. J. *Angew. Chem., Int. Ed.* **1998**, *37*, 1986.
(12) Krzemiński, M.; Wojtczak, A. *Tetrahedron Lett.* **2005**, *46*, 8299.
(13) Stepanenko, V.; Ortiz-Marciales, M.; Correa, W.; De Jesus, M.; Espinosa, S.; Ortiz, L. *Tetrahedron: Asymmetry* **2006**, *17*, 112.
(14) Krzemiński, M. P.; Ćwiklińska, M. *Tetrahedron Lett.* **2011**, *52*, 3919.
(15) (a) Huang, K.; Ortiz-Marciales, M.; Stepanenko, V.; Correa, W.; De Jesus, M. *J. Org. Chem.* **2008**, *73*, 6928. (b) Huang, K.; Merced, F. G.; Ortiz-Marciales, M.; Melendez, H. J.; Correa, W.; De Jesus, M. *J. Org. Chem.* **2008**, *73*, 4017. (c) Huang, X.; Ortiz-Marciales, M.; Huang, K.; Stepanenko, V.; Merced, F. G.; Ayala, A. M.; Correa, W.; De Jesus, M. *Org. Lett.* **2007**, *9*, 1793. (d) Chu, Y.; Shan, Z.; Liu, D.; Sun, N. *J. Org. Chem.* **2006**, *71*, 3998.
(16) Trost, B. M.; Terrell, L. R. *J. Am. Chem. Soc.* **2003**, *125*, 338.
(17) Li, G.; Chang, H. T.; Sharpless, K. B. *Angew. Chem., Int. Ed.* **1996**, *35*, 451.
(18) Bartoli, G.; Bosco, M.; Carlone, A.; Locatelli, M.; Massaccesi, M.; Melchiorre, P.; Sambri, L. *Org. Lett.* **2004**, *6*, 2173.
(19) Kureshy, R. I.; Singh, S.; Khan, N. H.; Abdi, S. H. R.; Agrawal, S.; Jasra, R. V. *Tetrahedron: Asymmetry* **2006**, *17*, 1638.
(20) Carrée, F.; Gil, R.; Collin, J. *Tetrahedron Lett.* **2004**, *45*, 7749.
(21) Harris, R. K.; Wasylishen, R. E.; Duer, M. J. *NMR Crystallography in Encyclopedia of Magnetic Resonance*; John Wiley & Sons Ltd: New York, 2009.
(22) (a) Küçükbenli, E.; Sonkar, K.; Sinha, N.; de Gironcoli, S. *J. Phys. Chem. A* **2012**, *116*, 3765. (b) Harris, R. K.; Hodgkinson, P.; Zorin, V.; Dumez, J.-N.; Elena-Herrmann, B.; Emsley, L.; Salager, E.; Stein, R. S. *Magn. Reson. Chem.* **2010**, *48*, S103. (c) Harris, R. K.; Cadars, S.; Emsley, L.; Yates, J. R.; Pickard, C. J.; Jetti, R. K. R.; Griesser, U. J. *Phys. Chem. Chem. Phys.* **2007**, *9*, 360.
(23) Benoit, M.; Profeta, M.; Mauri, F.; Pickard, C. J.; Tuckerman, M. E. *J. Phys. Chem. B* **2005**, *109*, 6052.
(24) Ashbrook, S. E.; Le Polles, L.; Gautier, R.; Pickard, C. J.; Walton, R. I. *Phys. Chem. Chem. Phys.* **2006**, *8*, 3423.
(25) Harris, R. K. *Analyst* **2006**, *131*, 351.
(26) Lister, S. E.; Soleilhavoup, A.; Withers, R. L.; Hodgkinson, P.; Evans, J. S. O. *Inorg. Chem.* **2010**, *49*, 2290.
(27) Fung, B. M.; Khitrin, A. K.; Ermolaev, K. *J. Magn. Reson.* **2000**, *142*, 97.
(28) Van Rossum, B.-J.; Förster, H.; De Groot, H. J. M. *J. Magn. Reson.* **1997**, *124*, 516.
(29) (a) Dvinskikh, S. V.; Zimmermann, H.; Maliniak, A.; Sandström, D. *J. Magn. Reson.* **2003**, *164*, 165. (b) Yamamoto, K.; Lee, D. K.; Ramamoorthy, A. *Chem. Phys. Lett.* **2005**, *407*, 289.
(30) *X-RED*, version 1.18; STOE & Cie GmbH: Darmstadt, Germany, 1999.
(31) Sheldrick, G. M. *Acta Crystallogr.* **2008**, *A64*, 112.
(32) (a) Clark, S. J.; Segall, M. D.; Pickard, C. J.; Hasnip, P. J.; Probert, M. J.; Refson, K.; Payne, M. C. *Z. Kristallogr.* **2005**, *220*, 567. (b) Segall, M. D.; Lindan, P. J. D.; Probert, M. J.; Pickard, C. J.; Hasnip, P. J.; Clark, S. J.; Payne, M. C. *J. Phys.: Condens. Matter* **2002**, *14*, 2717.
(33) Perdew, J. P.; Burke, K.; Ernzerhof, K. M. *Phys. Rev. Lett.* **1996**, *77*, 3865.
(34) Vanderbilt, D. *Phys. Rev. B* **1990**, *41*, 7892.
(35) Monkhorst, H. J.; Pack, J. D. *Phys. Rev. B* **1976**, *13*, 5188−5192.
(36) Pickard, C. J.; Mauri, F. *Phys. Rev. B* **2001**, *63*, 245101−245112.
(37) Webber, A. L.; Emsley, L.; Claramunt, R. M.; Brown, S. P. *J. Phys. Chem. A* **2010**, *114*, 10435.
(38) Cremer, D.; Pople, J. A. *J. Am. Chem. Soc.* **1975**, *97*, 1354.
(39) Duax, W. L.; Norton, D. A. *Atlas of Steroid Structures*; Plenum Press: London, U.K., 1975.
(40) Bialek, M.; Trzęsowska, A.; Kruszyński, R. *Bull. Korean Chem. Soc.* **2007**, *28*, 89.
(41) Desiraju, G. R.; Steiner, T. *The Weak Hydrogen Bond in Structural Chemistry and Biology*; Oxford University Press: Oxford, U.K., 1999.
(42) Yates, J. R.; Pham, T. N.; Pickard, C. J.; Mauri, F.; Amado, A. M.; Gil, A. M.; Brown, S. P. *J. Am. Chem. Soc.* **2005**, *127*, 10216.
(43) (a) Alla, M.; Lippmaa, E. *Chem. Phys. Lett.* **1976**, *37*, 260. (b) Opella, S. J.; Frey, M. H. *J. Am. Chem. Soc.* **1979**, *101*, 5854. (c) Zilm, K. W. In *Spectral Editing Techniques: Hydrocarbon Solids Encyclopedia of NMR*; Grant, D. M., Harris, R. K, Eds.; John Wiley & Sons Ltd: Chichester, U.K., 1996; Vol. *VII*, pp 4498−4504.
(44) Shao, L.; Yates, J. R.; Titman, J. J. *J. Phys. Chem. A* **2007**, *111*, 13126.
(45) Antzutkin, O. N.; Shekar, S. C.; Levitt, M. H. *J. Magn. Reson., Ser. A* **1995**, *115*, 7.
(46) (a) Pawlak, T.; Trzeciak-Karlikowska, K.; Czernek, J.; Ciesielski, W.; Potrzebowski, M. J. *J. Phys. Chem. B* **2012**, *116*, 1974. (b) Carignani, E.; Borsacchi, S.; Marini, A.; Mennucci, B.; Geppi, M. *J. Phys. Chem. C* **2011**, *115*, 25023. (c) Dumez, J. N.; Pickard, C. J. *J. Chem. Phys.* **2009**, *130*, 104701. (d) De Gortari, I.; Portella, G.; Salvatella, X.; Bajaj, V. S.; van der Wel, P. C.; Yates, J. R.; Segall, M. D.; Pickard, C. J.; Payne, M. C.; Vendruscolo, M. *J. Am. Chem. Soc.* **2010**, *132*, 5993.

(47) Harris, R. K.; Hodgkinson, P.; Pickard, C. J.; Yates, J. R.; Zorin, V. *Magn. Reson. Chem.* **2007**, *45*, S174.
(48) Bielecki, A.; Kolbert, A. C.; Levitt, M. H. *Chem. Phys. Lett.* **1989**, *155*, 341.
(49) Robinson, M.; Haynes, P. D. *J. Chem. Phys.* **2010**, *133*, 084109.
(50) Cadars, S.; Lesage, A.; Pickard, C. J.; Sautet, P.; Emsley, L. *J. Phys. Chem.* **2009**, *113*, 902.
(51) Marassi, F. M.; Opella, S. J. *J. Magn. Reson.* **2000**, *144*, 150.
(52) Pake, G. E. *J. Chem. Phys.* **1948**, *16*, 327.